ISSN 0027-1314, Moscow University Chemistry Bulletin, 2021, Vol. 76, No. 2, pp. 85–94. © Allerton Press, Inc., 2021.
Russian Text © The Author(s), 2021, published in Vestnik Moskovskogo Universiteta, Seriya 2: Khimiya, 2021, No. 3, pp. 179–191.

Physicochemical Properties of Aluminate Solutions

K. V. Rotmanov[a], *, ** and M. N. Smirnov[b], ***

[a] *AO State Scientific Centre, Research Institute of Nuclear Reactors, Dimitrovgrad, 433510 Russia*
[b] *Department of Physics and Technology, Dimitrovgrad Engineering and Technological Institute, National Research Nuclear University MEPhI (Moscow Engineering Physics Institute), Dimitrovgrad, 433511 Russia*
**e-mail: kvrotmanov@niiar.ru*
***e-mail: orip@niiar.ru*
****e-mail: mnsmirnov@niiar.ru*

Received May 10, 2020; revised May 12, 2020; accepted May 20, 2020

Abstract—This bibliographical review represents the published data on the composition and structure of aluminate ions in solutions with varied Al(III) and NaOH concentrations. The results of investigations of the partial and integral properties of aluminate solutions regarded as a ternary $NaOH–NaAl(OH)_4–H_2O$ system are given. The phase diagrams of the ternary $Na_2O–Al_2O_3–H_2O$ system for temperatures of 30, 95, 110, 130, 150, and 180°C are presented, and the compositions of the solid phases existing in equilibrium with the corresponding saturated aluminate solutions are specified.

Keywords: aluminate solutions, hydroxo forms, phase diagrams
DOI: 10.3103/S0027131421020097

INTRODUCTION

The properties of aluminate solutions is one of the most popular subjects of research in the chemistry of aluminum. Alkaline solutions are used in the alumina industry for the selective extraction of aluminum from bauxite ores. The production of alumina from aluminum feedstock by alkaline methods results in technological liquors among which the most typical ones are aluminate solutions contaminated with varied inorganic and organic impurities. In the case of using the Bayer method, they are obtained after leaching bauxites, and, in the case of using the sintering method, they are obtained after leaching aluminate sinters [1]. The properties of the aluminate solutions obtained by not only the Bayer method but also other alkaline methods of alumina production are largely determined by the technological process. For many years, the chemistry of sodium aluminate solutions has been studied in the context of the industrial processing of bauxite ores. However, recently this process has become especially important due to the urgency of the problems concerning radioactive waste (RAW). Alkaline RAW from defense programs occurs in the National Laboratories of the United States and at PO Mayak (Russia) [2, 3], with sodium aluminate and NaOH being the dominant components of the alkaline RAW [4, 5].

In this bibliographical review, most of the works deal with the so-called synthetic Bayer liquors, which are homogeneous and contain only H_2O, NaOH, and Al(III) hydroxo forms in their composition. The discussion does not cover aluminate solutions containing cations other than Na^+ (i.e., Li^+, K^+, and Cs^+). As was mentioned above, the technological aluminate solutions used in alumina production are intrinsically complex and multicomponent. However, in the study [4], it was demonstrated that the thermodynamic model of synthetic Bayer liquors can be a base for predicting the properties of real technological aluminate solutions.

The aim of this review is to consider the results of investigations of the physicochemical properties of the aluminate solutions currently available in the literature.

THE COMPOSITION AND STRUCTURE OF ALUMINATE IONS IN ALUMINATE SOLUTIONS

At present, aluminate solutions are considered as true (ionic) solutions. This supposition is corroborated by a large amount of experimental data on the behavior of sodium aluminate solutions [6–8]. Nevertheless, the issue as to the composition and structure of aluminate ions in solutions with different concentrations of alkali and aluminum has not yet been settled completely.

To solve the question about the composition and structure of aluminate ions, a wide range of spectroscopic methods was involved: Raman spectroscopy

[9–16], IR and UV spectroscopy [9–10, 14–15, 17–18], nuclear magnetic resonance (NMR) method [9, 11, 13, 17], X-ray spectroscopy methods [19], static and dynamic light scattering [20–23], and the dielectric relaxation technique [24–25]. In addition, electrochemical methods were used [11, 20–21, 26–28] (potentiometry, conductometry, linear voltammetry), and the rheological properties of aluminate solutions were investigated [21, 28–30]. Based on the results obtained in the works [9–30], we can declare that in all likelihood, in aluminate solutions, monomer tetrahydroxo aluminate ion $[Al(OH)_4]^-$ with a tetrahedral configuration and a dimer hydroxo form $Al_2O(OH)_6^{2-}$—exists.

It is considered practically a proven fact [6–8] that, in thermodynamically stable aluminate solutions unsaturated with [Al] (hereainfter in the text, square brackets in the designation of concentration of the solution component indicate its analytical concentration) and having a high pH value, singly charged mononuclear $[Al(OH)_4]^-$ aluminate ions are dominant. In [8], it is indicated that three types of monoaluminate ions in the form of singly charged anions with a differing degree of hydration can coexist in aluminate solutions:

$$[Al(OH)_4]^- \leftrightarrow [AlO(OH)_2]^- + H_2O$$
$$\leftrightarrow AlO_2^- + 2H_2O,$$

with this equilibrium shifting to the right with increasing temperature and [NaOH] and [Al] concentrations. The results of investigations of aluminate solutions obtained by Raman and IR spectroscopy ($0.5 < [Al] < 6$ mol/L; $1.25 < [NaOH] < 8.3$ mol/L) are presented in [9]. It is demonstrated that, at $[Al] < 1.5$ mol/L, the dominant form is $Al[(OH)_4]^-$; at $[Al] > 1.5$ mol/L, $[(OH)_3AlOAl(OH)_3]^{2-}$ dimer aluminate ions with one oxo bridge of the Al–O–Al type are formed in the solution:

$$[Al(OH)_4]^- + [Al(OH)_4]^-$$
$$\leftrightarrow [Al_2O(OH)_6]^{2-} + 2H_2O.$$

The authors of [9] confirm the fact of dehydration of an $[Al(OH)_4]^-$ ion with increasing [NaOH] and [Al] concentrations, albeit, with the subsequent formation of an $[Al_2O(OH)_6]^{2-}$ dimer complex rather than ions of the $[AlO(OH)_2]^-$ and AlO_2^- type.

In aluminate solutions, the formation of a measurable number of hydrated monoaluminate ions (such as $[AlO(OH)_2]^-$ or AlO_2^-), and higher hydroxocomplexes of the $[Al(OH)_5]^{2-}$ and $[Al(OH)_6]^{3-}$ form is disproved by the majority of the experimental data [6, 8]. Analysis of the data of Raman and IR spectroscopy of aluminate solutions carried out in [6, 8] made it possible to conclude that there are no aluminate ions formed by $[Al(OH)_4]^-$ oligomerization (apart from the $Al_2O(OH)_6]^{2-}$ dimer hydroxo form).

In the publications [8–9, 31], the formation of $Na^+Al(OH)_4^-$ ion associates (ion pairs) between sodium and aluminate ions was proven. Such associates are quite strong and can be qualified as outer sphere complexes [32]. In addition, it was established with confidence [33, 34] that there were Na^+OH^- ion pairs in NaOH solutions. In [8], it was mentioned that the concentration dependences of the electrical conductivity of aluminate solutions and NaOH solutions are symbatic and pass the maximum with an increasing concentration. The electrical conductivity of NaOH solutions decreases beyond the limits of complete solvation and is due to the decrease in the concentrations of Na^+ and OH^- ions because of the formation of ion associates (ion pairs) between sodium ions and hydroxy anions. An analogous view of the change in the electrical conductivity of aluminate solutions can also be caused by the formation of ion associates between aluminate anions, hydroxy anions, and sodium cations.

In [35], with the use of Raman spectroscopy and viscosimetry, the concentration regions of the change in the dominating aluminate forms in aluminate solutions supersaturated with [Al] (metastable) ([NaOH]/[Al] = 1.4–1.7) are distinguished. In the sodium aluminate solution at Al(III) concentration up to 2.0 to 2.2 mol/L, the $[Al(OH)_4]^-$ monomer is dominant. In the region of the Al(III) concentration of 2.0 to 4.5 mol/L, in solution, monomers of aluminate ions prevail and their dimer forms $[Al_2O(OH)_6]^{2-}$ start to be formed. However, as the authors of [35] note, these are not the monomers dealt with while discussing the range of the Al(III) concentrations up to 2.0 to 2.2 mol/L. At quite high concentrations (>2.0 mol/L [Al]), the process of association of Na^+ and $[Al(OH)_4]^-$ ions is intensified. Most probably, in the sodium aluminate solution, in the region of the Al(III) concentration of 2.0 to 4.5 mol/L at 25°C, hydrate-separated associates of $[Al(OH)_4]^-$ monomers with Na^+ cations are prevalent. In the Al(III) concentration range of 4.8 to 6.0 mol/L, dimer forms of an aluminate forming associates with Na^+ ions become dominant in solution [35]. The possibility of the outer sphere complexation of the dimer aluminate forms with Na^+ ions was also noted in [12, 13, 24, 25]. The results of investigations of the NMR and Raman spectra in alkaline aluminate solutions [12–13] and the processes of dielectric relaxation in these solutions [24–25] are evidence of the possibility of the existence of contact ion pairs of Na^+ and monomer and dimer forms of aluminate ions at [Al] = 0.8 mol/L and [NaOH] > 10 mol/L.

In the study [9], it was discovered that the IR, Raman, and NMR spectra of the aluminate solution (2 mol/L) containing monomer and dimer forms of aluminate ions do not alter at a temperature up to 150°C. In [12], it was established that the parameters of the Raman spectra of the aluminate solution ([Al] = 5.154 mol/L and [NaOH] = 8.183 mol/L) remain

nearly the same when the temperature is raised from 25 to 100°C. As the authors of [9, 12] assumed, equilibrium between the monomer and dimer hydroxo forms of aluminate ions weakly depends on temperature. As was noted in [8], the concentration of dimer aluminate ions is not so large as to noticeably affect the spectra. In [36], concentrated aluminate solutions ($1.6 < [Al] < 4.4$ mol/L; [NaOH]/[Al] = 1.5) were investigated at a temperature of 20 to 95°C by molecular spectroscopy (Raman, IR, and UV). The behavior of the parameters in the Raman, IR, and UV spectra leads us to state that an increase in temperature decreases the number of the monomer $[Al(OH)_4]^-$ species in aluminate solutions and encourages the growth in the number of dimer $[Al_2O(OH)_6]^{2-}$ or more complex species with Al–O–Al bonds [36].

The existence of polymer aluminate ions

$$\left([Al_2(OH)_2(H_2O)_4]^{4+},\right.$$
$$[Al_3(OH)_4(H_2O)_9]^{5+},$$
$$[Al_{13}O_4(OH)_{24}(H_2O)_{12}]^{7+},$$
$$\left.[Al_{30}O_8(OH)_{56}(H_2O)_{26}]^{18+}\right),$$

in solutions with different concentrations at pH 4–5 was reported in a series of publications [20, 37–39]. However, the data on the presence of polynuclear structures in strongly alkaline solutions (e.g., $[Al_6(OH)_{24}]^{6-}$ hexameric hydroxo forms [26, 28]) are controversial. Numerous published data [6, 11] do not confirm the presence of a noticeable number of polymer aluminate ions in strongly alkaline solutions.

As the author of [6] holds, the assumption that, there are only Na^+, OH^-, and an $[Al(OH)_4]^-$ dimer aluminate ion and ion pairs corresponding to them in the system, is quite sufficient for explaining the features of the behavior of concentrated alkaline aluminate solutions at a temperature up to 100°C.

PHYSICOCHEMICAL PROPERTIES OF ALUMINATE SOLUTIONS

An important role in the investigation of aluminate solutions is played by the physicochemical analysis based on plotting the temperature and concentration dependences of their thermodynamic (Gibbs free energy of mixing and enthalpy of mixing, heat capacity, and density) and other (refractive index and viscosity) physicochemical properties. The obtained experimental data are the base for building the thermodynamic models of aluminate solutions. In the majority of the presented publications, as a thermodynamic model, the Pitzer model for concentrated electrolyte solutions is used [40] and aluminate solutions are regarded as the $NaOH–NaAl(OH)_4–H_2O$ system.

The results of the experimental studies of the integral and partial properties of aluminate solutions are given in [41–59]. The standard partial molar volume of an $Al(OH)_4^-$ (aq) ion in an infinitely dilute aqueous solution at a temperature of 25°C [41] and the standard molar enthalpy and the standard molar Gibbs free energy of formation of an $Al(OH)_4^-$ (aq) ion in an infinitely dilute aqueous solution in the temperature range of 0–160°C are determined [42–43].

The values of the viscosity, density, and refractive index for the sodium aluminate solutions ($[Al] \le 4.38$ mol/L, $[NaOH] \le 6$ mol/L, $1.37 \le [NaOH]/[Al] \le 26.67$) are established at a temperature of 22 to 75°C [44].

The values of the viscosity and density for the sodium aluminate solutions ($[NaOH] \le 13.6$ mol/kg H_2O and $[Al(III)]/[Na^+] \le 0.6$) at 25°C for a series of solutions with the same ionic strength are determined [45].

The apparent molar heat capacity and apparent molar volume of concentrated sodium aluminate solutions at a temperature from 10 to 55°C are determined.

Based on the resulting data, the parameters of the Pitzer model were determined, which made it possible to calculate the standard partial molar heat capacity and standard partial molar volume for the $Al(OH)_4^-$ (aq) ion in the studied temperature range [46].

The apparent molar heat capacity of sodium aluminate solutions at a temperature of 323.15 to 523.15 K, a total molality of the solutions in the range of 0 to 1.7 mol/kg H_2O, and a pressure of 2.0 to 4.7 MPa [47] was measured.

The isobaric specific heat capacity (J/(g K)) and apparent molar heat capacity (J/(mol K)) of sodium aluminate solutions ($0.4 \le [NaOH] \le 6.0$ mol/kg H_2O; $0.1 \le [Al] \le 3.0$ mol/kg H_2O; $0 \le [Al]/[NaOH] \le 1.5$) at a total ionic strength (I) in the range of $1 < I < 6$ mol/kg H_2O at 298.15 K were measured [48].

Using the isopiestic method, the osmotic coefficients for the $NaOH–NaAl(OH)_4–H_2O$ system with the total molal concentration of $0.05 \le [NaOH] \le 12$ mol/kg H_2O ([NaOH]/[Al] = 1.64–5.53) at 313.2 K were determined [49]. Based on the results, the parameters of the Pitzer model were determined, which made it possible to calculate the mean ionic activity coefficients for NaOH and $NaAl(OH)_4$ and the H_2O activity for the $NaOH–NaAl(OH)_4–H_2O$ system in the investigated [NaOH] and [NaOH]/[Al] ranges.

Isopiestic measurements were carried out for the sodium aluminate solutions at 323.15 and 373.15 K, and the osmotic coefficients were determined for the $NaOH–NaAl(OH)_4–H_2O$ system. It was shown that this system obeys Zdanovskii's Rule [50]. For the sodium aluminate solutions, the density [51] and the values of the apparent molar heat capacity [52] at the total ionic strength of $1 \le I \le 6$ mol/kg H_2O and the sodium aluminate concentration in the range from 0.1 to 2.4 mol/kg H_2O in the temperature range of 323 to 573 K and a pressure of 10 MPa were determined.

In [53], the density of sodium aluminate solutions was measured in isomolal series at the total ionic strength in the range of $1 \le I \le 6$ mol/kg H_2O and the proportion between the concentrations of $0 \le [Al]/[NaOH] \le 0.6$ in the temperature range of $50°C \le T \le 90°C$ [53].

In [54], to forecast the density of the NaOH–$NaAl(OH)_4$–H_2O system, the Laliberté–Cooper model was used [55]. In addition, in [54], the parameters of the Laliberté–Cooper model were calculated, which made it possible to satisfactorily predict the density of sodium aluminate solutions in the temperature range of $25°C \le T \le 90°C$; and the mass fraction of the components of the system changed within the following limits: the mass fraction of NaOH changed from 0.0039 to 0.3534, that of $NaAl(OH)_4$ changed from 0.0014 to 0.2793, and that of H_2O changed from 0.4858 to 0.9944.

Based on the available published data on the thermodynamic properties of sodium aluminate solutions, in [4, 56–58], a thermodynamic model of the liquid phase in the NaOH–$NaAl(OH)_4$–H_2O system was proposed. The Pitzer model was employed as a thermodynamic model of the solutions in the studied system. In [4, 56–58], the parameters of the Pitzer model were determined, which made it possible to calculate the partial and integral properties of solutions in the NaOH–$NaAl(OH)_4$–H_2O system in the scale of molal concentrations.

Due to the great technological significance of aluminate solutions, experimental investigations of the solubility of aluminum hydroxide in caustic soda depending on the concentration of the components and temperature were repeatedly carried out [59–62]. Nevertheless, despite the fact that investigation of the solubility of isotherms of aluminum hydroxide in caustic soda is dealt with in many publications, this investigation still cannot be deemed completed. In relatively recent studies [63–66], the isotherms of the solubility of aluminum hydroxide in caustic soda were plotted for temperatures of 30, 95, 110, 130, 150, and 180°C, and the compositions of the solid phases existing in equilibrium with the corresponding saturated aluminate solutions were specified.

The authors of [63–66] used a conventional form of representation of the composition of aluminate solutions: the concentrations were recalculated (in weight fractions or percent) for the components of the aluminate solution (of alkali and aluminum hydroxide) into Na_2O and Al_2O_3 oxides [59]. Therefore, in the publications [63–66], the phase diagrams of the Na_2O–Al_2O_3–H_2O ternary system are considered.

In [63–66], for imaging the composition of the Na_2O–Al_2O_3–H_2O system, the first Roseboom's technique was employed: the composition of the ternary system was depicted with an isosceles right triangle [67]. The vertex of the right angle corresponds to a pure solvent (H_2O) and the values of the Na_2O concentration (abscissa axis) and Al_2O_3 (ordinate axis) were plotted along the cathetuses of the triangle. The area of the phase diagram limited by the solubility curves and connecting straight lines (connodes) is divided into several fields, with each field corresponding to the composition of the mixtures answering the coexistence of certain phases. In the phase diagram reported in [63–66], only the so-called aqueous angle, whose vertex is a point of H_2O is represented and not the whole Roseboom triangle.

In [63], phase equilibria are investigated in the Na_2O–Al_2O_3–H_2O system for 30°C in the region with a high Na_2O content. The phase diagram of the Na_2O–Al_2O_3–H_2O system for 30°C is shown in Fig. 1a.

Under these conditions in the system, as solid phases, gibbsite $Al_2O_3 \cdot 3H_2O$ ($Al(OH)_3$) (point A), sodium hydroaluminates $Na_2O \cdot Al_2O_3 \cdot 2.5H_2O$ (point B) and $4Na_2O \cdot Al_2O_3 \cdot 12H_2O$ (point C), and caustic soda monohydrate $NaOH \cdot H_2O$ ($Na_2O \cdot 3H_2O$) (point D) crystallize. The solubility curve KJFG (the region with a high Na_2O content) in the isotherm of the ternary system consists of branches KJ, JF, and FG, intersecting at invariant points K, J, and F, corresponding to the coexistence of three phases. The compositions of the phases in the invariant points are presented in Table 1. Point G on the abscissa axis (Fig. 1b) shows the solubility of $NaOH \cdot H_2O$ in pure water at 30°C, which is 42.10 wt % Na_2O in the NaOH–H_2O system [68]. Branches KJ, JF (Fig. 1a), and FG (Fig. 1b) of the solubility curve reflect the compositions of the unsaturated solutions existing in equilibrium with, correspondingly, $Na_2O \cdot Al_2O_3 \cdot 2.5H_2O$ (point B), $4Na_2O \cdot Al_2O_3 \cdot 12H_2O$ (point C), and $Na_2O \cdot 3H_2O$ ($NaOH \cdot H_2O$) (point D) solid phases.

The ABKA, BCJB, and CDFC regions are three-phase regions of the coexistence of, respectively, $Al_2O_3 \cdot 3H_2O$ ($Al(OH)_3$) (point A), $Na_2O \cdot Al_2O_3 \cdot 2.5H_2O$ (point B), and a solution saturated with these solid phases (point K); $Na_2O \cdot Al_2O_3 \cdot 2.5H_2O$ (point B), $4Na_2O \cdot Al_2O_3 \cdot 12H_2O$ (point C), and a solution saturated with these solid phases (point J); $4Na_2O \cdot Al_2O_3 \cdot 12H_2O$ (point C), $Na_2O \cdot 3H_2O$ ($NaOH \cdot H_2O$) (point D), and a solution saturated with these solid phases (point F). The region above the ABCD line corresponds to a completely crystallized system, and the region below the KJFG line corresponds to the existence of unsaturated aluminate solutions.

In Fig. 2, the solubility curves for 30°C in the region with a high Na_2O content obtained in the early study [69] and study [63] where the phase diagram of the Na_2O–Al_2O_3–H_2O system for 30°C was investigated again were compared. In [63], the equilibrium composition of the aluminate solution at the invariant point K was specified (Table 1) to be 21.02 wt % Na_2O and 19.01 wt % Al_2O_3, unlike the composition

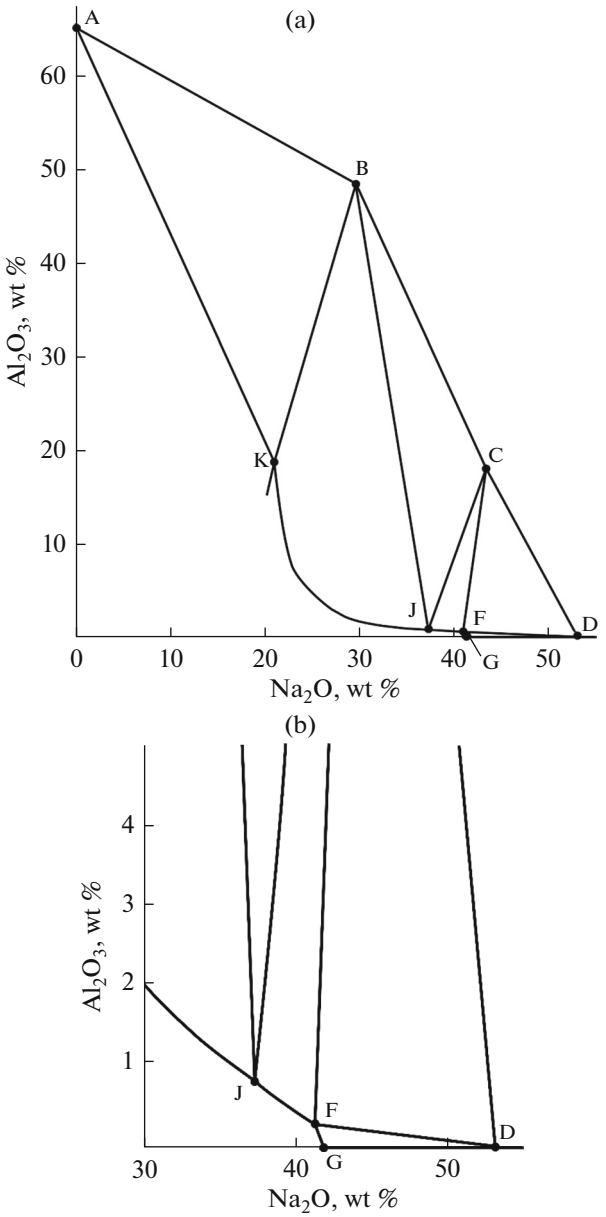

Fig. 1. Phase diagram of the Na_2O–Al_2O_3—H_2O system for 30°C: (a) general view of the phase diagram of the Na_2O–Al_2O_3—H_2O system for 30°C; (b) fragment of the phase diagram of the Na_2O–Al_2O_3—H_2O system for 30°C in the region with a high Na_2O content.

(21.95 wt % Na_2O and 25.59 wt % Al_2O_3) earlier reported in [69].

The phase diagram of the Na_2O–Al_2O_3–H_2O system for 95°C [64] is illustrated in Fig. 3. Under these conditions in the system, as solid phases, gibbsite $Al_2O_3·3H_2O$ ($Al(OH)_3$) (point A), sodium hydroaluminates $Na_2O·Al_2O_3·2.5H_2O$ (point B), $4Na_2O·Al_2O_3·12H_2O$ (point C), $6Na_2O·Al_2O_3·12H_2O$ (point D), and $Na_2O·H_2O$ (NaOH) (point E) crystallize. Correspondingly, the solubility curve OKJIFG in

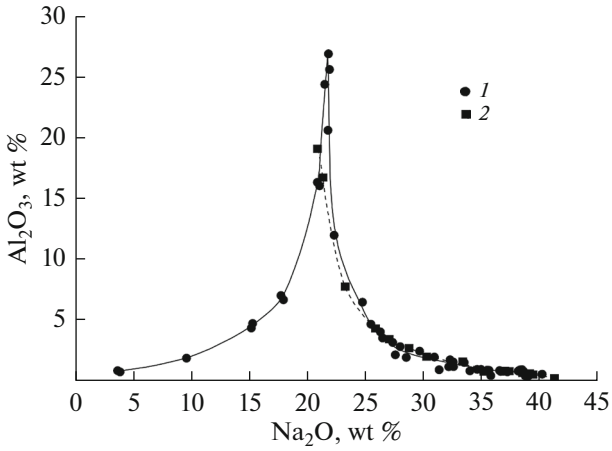

Fig. 2. Comparison of the solubility curves for 30°C in the region with a high Na_2O content obtained in studies (*1*) [63] and (*2*) [69].

the isotherm of the ternary system breaks up into five branches (according to the number of solid phases in the system). The solubility curve OKJIFG consists of branches OK, KJ, JI, IF, and FG, intersecting at the invariant points K, J, I, and F, corresponding to the coexistence of three phases. The compositions of the phases at the invariant points are presented in Table 1.

Point O on the ordinate axis of the diagram shows the solubility of $Al_2O_3·3H_2O$ ($Al(OH)_3$) in pure water (some data on the gibbsite solubility in water and dilute electrolyte solutions are presented in [70, 71]) at 95°C, and point G on the abscissa axis is the solubility of $Na_2O·H_2O$ (NaOH) in pure water at 95°C, which is 59.58 wt % Na_2O in the NaOH–H_2O system. The branches OK, KJ, JI, IF, and FG of the solubility curve (unfortunately, the scale of the phase diagrams reported in [64–66] and illustrated in Figs. 3–5 does not allow us to clearly reproduce branch FG) represent the compositions of the saturated solutions existing in equilibrium with, correspondingly, the $Al_2O_3·3H_2O$ (point A), $Na_2O·Al_2O_3·2.5H_2O$ (point B), $4Na_2O·Al_2O_3·12H_2O$ (point C), $6Na_2O·Al_2O_3·12H_2O$ (point D), and $Na_2O·H_2O$ (NaOH) (point E) solid phases.

The ABKA, BCJB, CDIC, and DEFD areas are three-phase regions of the coexistence of, respectively, $Al_2O_3·3H_2O$ (point A), $Na_2O·Al_2O_3·2.5H_2O$ (point B), and a solution saturated with both solid phases (point K); $Na_2O·Al_2O_3·2.5H_2O$ (point B), $4Na_2O·Al_2O_3·12H_2O$ (point C), and a solution saturated with these solid phases (point J); $4Na_2O·Al_2O_3·12H_2O$ (point C), $6Na_2O·Al_2O_3·12H_2O$ (point D), and a solution saturated with these solid phases (point I); and $6Na_2O·Al_2O_3·12H_2O$ (point D), $Na_2O·H_2O$ (NaOH), and a solution saturated with these solid phases (point F). The region above the ABCDE line corresponds to the completely crystallized system, and the region below

Table 1. Invariant points in the $Na_2O–Al_2O_3–H_2O$ system

Temperature, °C	Invariant point*	Composition of the equilibrium liquid phase		Equilibrium solid phases
		Na_2O, wt %	Al_2O_3, wt %	
30	K	21.02	19.01	$Al_2O_3·3H_2O + Na_2O·Al_2O_3·2.5H_2O$
	J	37.46	0.82	$Na_2O·Al_2O_3·2.5H_2O + 4Na_2O·Al_2O_3·12H_2O$
	F	41.23	0.25	$4Na_2O·Al_2O_3·12H_2O + Na_2O·3H_2O$ ($NaOH·H_2O$)
95	K	20.93	27.21	$Al_2O_3·3H_2O + Na_2O·Al_2O_3·2.5H_2O$
	J	42.12	2.10	$Na_2O·Al_2O_3·2.5H_2O + 4Na_2O·Al_2O_3·12H_2O$
	I	51.27	0.31	$4Na_2O·Al_2O_3·12H_2O + 6Na_2O·Al_2O_3·12H_2O$
	F	59.70	0.11	$6Na_2O·Al_2O_3·12H_2O + Na_2O·H_2O$ (NaOH)
110	K	23.72	29.37	$Al_2O_3·3H_2O + Na_2O·Al_2O_3·2.5H_2O$
	J	55.23	0.46	$Na_2O·Al_2O_3·2.5H_2O + 6Na_2O·Al_2O_3·12H_2O$
	F	60.80	0.20	$6Na_2O·Al_2O_3·12H_2O + Na_2O·H_2O$ (NaOH)
130	K	22.54	29.43	$Al_2O_3·H_2O + Na_2O·Al_2O_3·2.5H_2O$
	E	37.71	7.48	$Na_2O·Al_2O_3·2.5H_2O + Na_2O·Al_2O_3$
	F	61.45	0.38	$Na_2O·Al_2O_3 + Na_2O·H_2O$ (NaOH)
150	K	24.05	33.58	$Al_2O_3·H_2O + Na_2O·Al_2O_3·2.5H_2O$
	E	33.78	15.97	$Na_2O·Al_2O_3·2.5H_2O + Na_2O·Al_2O_3$
	F	61.56	0.43	$Na_2O·Al_2O_3 + Na_2O·H_2O$ (NaOH)
180	K	25.09	35.86	$Al_2O_3·H_2O + Na_2O·Al_2O_3·2.5H_2O$
	E	30.82	25.82	$Na_2O·Al_2O_3·2.5H_2O + Na_2O·Al_2O_3$
	F	61.96	0.12	$Na_2O·Al_2O_3 + Na_2O·H_2O$ (NaOH)

* Positions of invariant points at temperatures of 30, 95, 110, 130, 150, and 180°C are shown in Figs. 1, 3–5.

the OKJIFG line corresponds to the existence of unsaturated aluminate solutions in the system.

The phase diagram of the $Na_2O–Al_2O_3–H_2O$ system for 110°C [64] is represented in Fig. 4. Under these conditions in the system, as solid phases, gibbsite $Al_2O_3·3H_2O$ ($Al(OH)_3$) (point A), sodium hydroaluminates $Na_2O·Al_2O_3·2.5H_2O$ (point B) and $6Na_2O·Al_2O_3·12H_2O$ (point D), and $Na_2O·H_2O$ (NaOH) (point E) crystallize. Correspondingly, the solubility curve OKJFG in the isotherm of the ternary system breaks up into four branches (according to the number of solid phases in the system). The solubility curve OKJFG consists of branches OK, KJ, JF, and FG, intersecting at the invariant points K, J, and F, corresponding to the coexistence of three phases. The compositions of phases at invariant points are presented in Table 1.

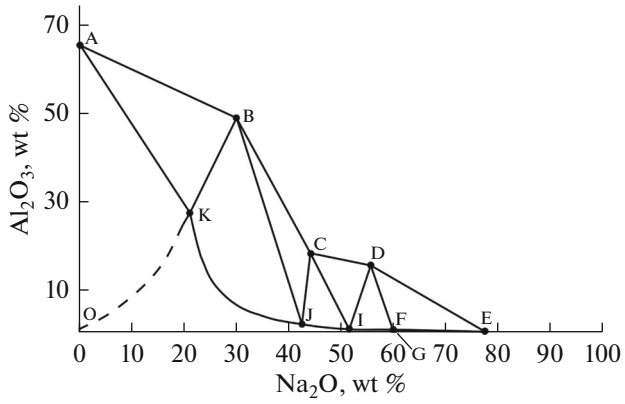

Fig. 3. Phase diagram of the $Na_2O–Al_2O_3–H_2O$ system for 95°C.

Point O on the ordinate axis of the diagram shows the solubility of $Al_2O_3·3H_2O$ ($Al(OH)_3$) in pure water at a temperature of 110°C, and point G on the abscissa axis shows the solubility of $Na_2O·H_2O$ (NaOH) in pure water at 110°C, which is 60.62 wt % Na_2O in the $NaOH–H_2O$ system. The branches OK, KJ, JF, and FG of the solubility curve reflect the composition of the saturated solution existing in equilibrium with, respec-

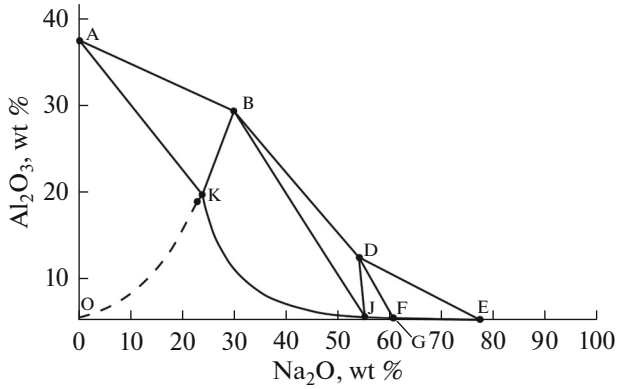

Fig. 4. Phase diagram of the $Na_2O–Al_2O_3–H_2O$ system for 110°C.

tively, $Al_2O_3·3H_2O$ (point A), $Na_2O·Al_2O_3·2.5H_2O$ (point B), $6Na_2O·Al_2O_3·12H_2O$ (point D), and $Na_2O·H_2O$ (NaOH) (point E) solid phases. The ABKA, BDJB, and DEFD regions are the three-phase regions of coexistence of, respectively, $Al_2O_3·3H_2O$ (point A), $Na_2O·Al_2O_3·2.5H_2O$ (point B), and a solution saturated with these solid phases (point K); $Na_2O·Al_2O_3·2.5H_2O$ (point B), $6Na_2O·Al_2O_3·12H_2O$ (point D), and a solution saturated with these solid phases (point J); and $6Na_2O·Al_2O_3·12H_2O$ (point D), Na_2O H_2O (NaOH) (point E), and a solution saturated with these solid phases (point F). The region above the ABDE line corresponds to the completely crystallized system, and the region below the OKJFG corresponds to the existence of unsaturated aluminate solutions in the system.

The solubility diagrams of the $Na_2O–Al_2O_3–H_2O$ system for 130, 150, and 180°C [65, 66] are presented in Fig. 5. Under these conditions in the system, as solid phases, $Al_2O_3·H_2O$ (AlOOH) (point A), sodium hydroaluminate $Na_2O·Al_2O_3·2.5H_2O$ (point B), anhydrous sodium aluminate $Na_2O·Al_2O_3$ ($NaAlO_2$) (point C), and $Na_2O·H_2O$ (NaOH) (point D) are crystallized. Correspondingly, the solubility curve OKEFG in the isotherm of the ternary system breaks up into four branches (according to the number of solid phases in the system). The solubility curve OKEFG consists of branches OK, KE, EF, and FG, intersecting at the invariant points K, E, and F, corresponding to the coexistence of three phases. The compositions of phases at the invariant points are presented in Table 1.

Point O on the ordinate axis of the diagram indicates the solubility of $Al_2O_3·H_2O$ (AlOOH) in pure water at the given temperature (some data on the boehmite solubility in water and dilute electrolyte solutions are presented in [72–74]), and point G on the ordinate axis shows the solubility of $Na_2O·H_2O$ (NaOH) in pure water, which is 61.42 wt % Na_2O at

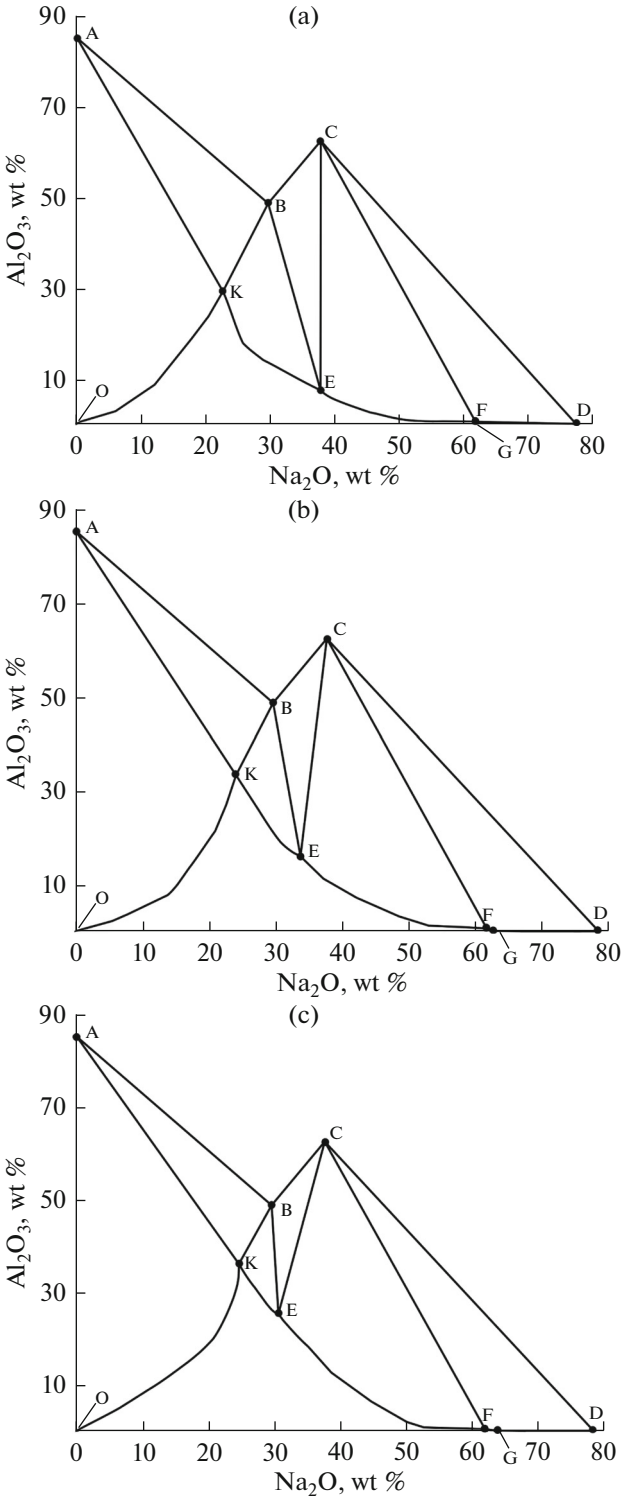

Fig. 5. Phase diagrams of the $Na_2O–Al_2O_3–H_2O$ system for temperatures of (a) 130, (b) 150, and (c) 180°C.

130°C, 62.38 wt % Na_2O at 150°C, and 64.00 wt % Na_2O at 180°C in the $NaOH–H_2O$ system.

Branches OK, KE, EF, and FG of the solubility curve reflect the composition of saturated solutions in

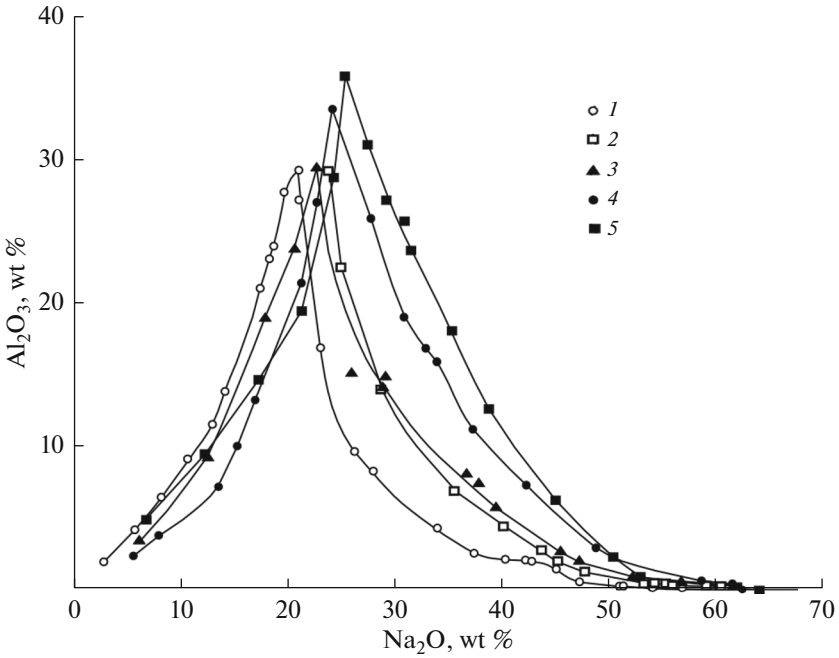

Fig. 6. Phase diagrams of the Na_2O–Al_2O_3–H_2O system at temperatures of [4, 57–59] (*1*) 95, (*2*) 110, (*3*) 130, (*4*) 150, and (*5*) 180°C.

equilibrium with, respectively, the $Al_2O_3 \cdot H_2O$ (AlOOH) (point A), $Na_2O \cdot Al_2O_3 \cdot 2.5H_2O$ (point B), $Na_2O \cdot Al_2O_3$ (point C), and $Na_2O \cdot H_2O$ (NaOH) (point D) solid phases.

The ABKA, BCEB, and CDFC regions are three-phase regions of the coexistence of, respectively, $Al_2O_3 \cdot H_2O$ (AlOOH) (point A), $Na_2O \cdot Al_2O_3 \cdot 2.5H_2O$ (point B), and a solution saturated with these solid phases (point K); $Na_2O \cdot Al_2O_3 \cdot 2.5H_2O$ (point B), $Na_2O \cdot Al_2O_3$ (point C), and a solution saturated with these solid phases (point E); and $Na_2O \cdot Al_2O_3$ (point C), $Na_2O \cdot H_2O$ (NaOH) (point D), and a solution saturated with these solid phases (point F). The region above the ABCD line corresponds to the completely crystallized system, and the region below the OKEFG line corresponds to the existence of unsaturated aluminate solutions in the system.

The data presented in Fig. 5 indicate that, with an increase in temperature, the KE branches of the solubility curves, reflecting the composition of saturated solutions existing in equilibrium with $Na_2O \cdot Al_2O_3 \cdot 2.5H_2O$ (point B), shorten; correspondingly, the EF branches of the solubility curves, reflecting the composition of saturated solutions which are in equilibrium with $Na_2O \cdot Al_2O_3$ (point C), lengthen. As the authors of [66] hold, this is evidence that, in concentrated alkaline solutions, with an increasing temperature, the content of sodium hydroaluminate in a precipitate decreases and anhydrous sodium aluminate $Na_2O \cdot Al_2O_3$ ($NaAlO_2$) becomes the dominant solid phase.

Figure 6 shows four isotherms of the Al_2O_3–Na_2O–H_2O system for 95, 130, 150, and 180°C. The shape of the isotherms is typical: the curves have an acute maximum, whose value is the maximum Al_2O_3 concentration in the equilibrium solution. From Fig. 6, it is seen that, with increasing temperature, the height of the maximums in the isotherms rises; in other words, with an increase in temperature, equilibrium solutions with a higher maximum Al_2O_3 concentration can be obtained. With an increasing temperature, the maximums of the isotherms shift toward higher Na_2O concentrations. Therefore, in order to obtain solutions with the maximum Al_2O_3 content, it is necessary to increase the Na_2O concentration simultaneously with increasing temperature.

Note that the data on the transformation of the solubility isotherm of the Al_2O_3–Na_2O–H_2O system with an increasing temperature obtained in [63–66] agree well with the results presented earlier in [59, 60].

CONFLICT OF INTEREST

The authors declare that they have no conflicts of interest.

SUPPLEMENTARY MATERIALS

There are no supplementary materials.

REFERENCES

1. Abramov, V.Ya., Stel'makova, G.D., and Nikolaev, I.V., *Fiziko-khimicheskie osnovy kompleksnoi pererabotki aly-*

uminievogo syr'ya (shchelochnye metody) (Physicochemical Fundamentals of Complex Processing of Aluminum Raw Materials (Alkaline Methods)), Moscow: Metallurgiya, 1985.

2. *Problemy yadernogo naslediya i puti ikh resheniya* (Nuclear Legacy Problems and Their Solutions), Evstratov, E.V., Agapov, A.M., Laverov, N.P., Bol'shov, L.A., and Linge, I.I., Eds., Moscow: Energopromanalitika, 2012, vol. 1.
3. Johnston, C.F., Agnew, S.F., Schoonover, J.R., Kenney, J.W., Page, B., Osborn, J., and Corbin, R., *Environ. Sci. Technol.*, 2002, vol. 36, no. 11, p. 2451.
4. Königsberger, E., Hefter, G., and May, P.M., Solubility of solids in Bayer liquors, in *Developments and Applications in Solubility*, Letcher, T.M., Ed., Cambridge: R. Soc. Chem., 2007, p. 236.
5. Reynolds, J.G., McCoskey, J.K., and Herting, D.L., *Ind. Eng. Chem. Res.*, 2016, vol. 55, no. 19, p. 5465.
6. Sipos, P., *J. Mol. Liq.*, 2009, vol. 146, nos. 1–2, p. 1.
7. Loginova, I.V., Shoppert, A.A., Rogozhnikov, D.A., and Kyrchikov, A.V., *Proizvodstvo glinozema i ekonomicheskie raschety v tsvetnoi metallurgii: uchebnoe posobie* (Alumina Production and Economic Calculations in Nonferrous Metallurgy: Textbook), Yekaterinburg: Ural Fed. Univ., 2016.
8. Eremin, N.I., Volokhov, Yu.A., and Mironov, V.E., *Russ. Chem. Rev.*, 1974, vol. 43, p. 92.
9. Moolenaar, R.J., Evans, J.C., and McKeever, L.D., *J. Phys. Chem.*, 1970, vol. 74, no. 20, p. 3629.
10. Ma, S., Zheng, S., Xu, H., and Zhang, Y., *Trans. Nonferrous Met. Soc. China*, 2007, vol. 17, no. 4, p. 853.
11. Sipos, P., Schibeci, M., Peintler, G., May, P., and Hefter, G., *Dalton Trans.*, 2006, no. 15, p. 1858.
12. Sipos, P., May, P., and Hefter, G., *Dalton Trans.*, 2006, no. 2, p. 368.
13. Sipos, P., Hefter, G., and May, P., *Talanta*, 2006, vol. 70, no. 4, p. 761.
14. Watling, H., Fleming, S., Bronswijk, W., and Rohl, A., *J. Chem. Soc., Dalton Trans.*, 1998, no. 23, p. 3911.
15. Chen, Y., Feng, Q., Liu, K., Chen, Y., and Zhang, G., *Chem. Phys. Lett.*, 2006, vol. 422, nos. 4–6, p. 406.
16. Rudolph, W.W. and Hefter, G.T., *Anal. Methods*, 2009, vol. 1, no. 2, p. 132.
17. Sipos, P., Capewell, S.G., May, P.M., Hefter, G., Laurenczy, G., Lukacs, F., and Roulet, R., *J. Chem. Soc., Dalton Trans.*, 1998, no. 18, p. 3007.
18. Li, X., Wang, D., Zhou, Q., Liu, G., and Peng, Z., *Hydrometallurgy*, 2011, vol. 106, nos. 1–2, p. 93.
19. Radnai, T., May, P., Hefter, G., and Sipos, P., *J. Phys. Chem. A*, 1998, vol. 102, no. 40, p. 7841.
20. Perry, C. and Shafran, K., *J. Inorg. Biochem.*, 2001, vol. 87, nos. 1–2, p. 115.
21. Li, J., Prestidge, C.A., and Addai-Mensah, J., *J. Colloid Interface Sci.*, 2000, vol. 224, no. 2, p. 317.
22. Soar, T., Counter, J., and Gerson, A., *Langmuir*, 2000, vol. 16, no. 11, p. 4784.
23. Li, H., Addai-Mensah, J., Thomas, J.C., and Gerson, A.R., *Colloids Surf., A*, 2003, vol. 223, nos. 1–3, p. 83.
24. Buchner, R., Hefter, G., May, P.M., and Sipos, P., *J. Phys. Chem. B*, 1999, vol. 103, no. 50, p. 11186.
25. Buchner, R., Sipos, P., Hefter, G., and May, P.M., *J. Phys. Chem. A*, 2002, vol. 106, no. 28, p. 6527.
26. Barcza, L. and Pálfalvi-Rózsahegyi, M., *Mater. Chem. Phys.*, 1989, vol. 21, no. 4, p. 345.
27. Sipos, P., Hefter, G., and May, P.M., *Aust. J. Chem.*, 1998, vol. 51, no. 6, p. 445.
28. Buvári-Barcza, A., Rózsahegyi, M., and Barcza, L., *J. Mater. Chem.*, 1998, vol. 8, no. 2, p. 451.
29. Addai-Mensah, J., Li, J., and Prestidge, C.A., *Asia-Pac. J. Chem. Eng.*, 2002, vol. 10, nos. 5–6, p. 553.
30. Addai-Mensah, J., Li, J., and Prestidge, C.A., *Asia-Pac. J. Chem. Eng.*, 2002, vol. 10, nos. 5–6, p. 539.
31. Diakonov, I., Pokrovski, G., Schott, J., Castet, S., and Gout, R., *Geochim. Cosmochim. Acta*, 1996, vol. 60, no. 2, p. 197.
32. Lukomskii, Yu.Ya. and Gamburg, Yu.D., *Fiziko-Khimicheskie osnovy elektrokhimii: uchebnoe posobie* (Physical and Chemical Foundations of Electrochemistry: Textbook), Dolgoprudnyi: Intellekt, 2013.
33. Megyes, T., Balint, S., Grosz, T., Radnai, T., Bako, I., and Sipos, P., *J. Chem. Phys.*, 2008, vol. 128, no. 4.
34. Moskovits, M. and Michaelian, K.H., *J. Am. Chem. Soc.*, 1980, vol. 102, no. 7, p. 2209.
35. Myund, L.A., Sizyakov, V.M., Khripun, M.K., and Makarov, A.A., *Zh. Obshch. Khim.*, 1995, vol. 65, no. 6, p. 911.
36. Myund, L.A., Sizyakov, V.M., Burkov, K.A., Zakharzhevskaya, V.O., and Borzenko, O.A., *Zh. Prikl. Khim.*, 1995, vol. 68, no. 12, p. 1964.
37. Bottero, J.Y., Cases, J.M., Flessinger, F., and Polrier, J.E., *J. Phys. Chem.*, 1980, vol. 84, no. 22, p. 2933.
38. Bottero, J.Y., Axelos, M., Tchoubar, D., Cases, J.M., Fripiat, J.J., and Flessinger, F., *J. Colloid Interface Sci.*, 1987, vol. 117, no. 1, p. 47.
39. Fournier, A.C., Shafran, K.L., and Perry, C.C., *Anal. Chim. Acta*, 2008, vol. 607, no. 1, p. 61.
40. *Activity Coefficients in Electrolyte Solutions*, Pitzer, K.S., Ed., Boca Raton: CRC, 1991, 2nd ed.
41. Sanjuan, B. and Michard, G., *J. Chem. Eng. Data*, 1988, vol. 33, no. 2, p. 78.
42. Chen, Q., Xu, Y., and Hepler, L.G., *Can. J. Chem.*, 1991, vol. 69, no. 11, p. 1685.
43. Zeng, W., Chen, Q., and Chen, X., *J. Chem. Thermodyn.*, 1994, vol. 26, no. 2, p. 205.
44. Li, J., Prestidge, C.A., and Addai-Mensah, J., *J. Chem. Eng. Data*, 2000, vol. 45, no. 4, p. 665.
45. Sipos, P., Stanley, A., Bevis, S., Hefter, G., and May, P.M., *J. Chem. Eng. Data*, 2001, vol. 46, no. 3, p. 657.
46. Hovey, J.K. and Hepler, L.G., *J. Phys. Chem.*, 1988, vol. 92, no. 5, p. 1323.
47. Caiani, P., Conti, G., Gianni, P., and Matteoli, E., *J. Solution Chem.*, 1989, vol. 18, no. 5, p. 447.
48. Magalhaes, M., Königsberger, E., May, P.M., and Hefter, G., *J. Chem. Eng. Data*, 2002, vol. 47, no. 4, p. 960.
49. Zhou, J., Chen, Q.Y., Li, J., Yin, Z.L., Zhou, X., and Zhang, P.M., *Geochim. Cosmochim. Acta*, 2003, vol. 67, no. 18, p. 3459.

50. Königsberger, E., Königsberger, L., Hefter, G., and May, P.M., *J. Solution Chem.*, 2007, vol. 36, nos. 11–12, p. 1619.
51. Schrödle, S., Königsberger, E., May, P.M., and Hefter, G., *Geochim. Cosmochim. Acta*, 2010, vol. 74, no. 8, p. 2368.
52. Hnědkovský, L., Königsberger, E., Königsberger, L., Cibulka, I., Schrödle, S., May, P.M., and Hefter, G., *J. Chem. Eng. Data*, 2010, vol. 55, no. 3, p. 1173.
53. Königsberger, E., Bevis, S., Hefter, G., and May, P.M., *J. Chem. Eng. Data*, 2005, vol. 50, no. 4, p. 1270.
54. Reynolds, J.G. and Carter, R., *Hydrometallurgy*, 2007, vol. 89, nos. 3–4, p. 233.
55. Laliberte, M. and Cooper, W.E., *J. Chem. Eng. Data*, 2004, vol. 49, no. 5, p. 1141.
56. Königsberger, E., Eriksson, G., May, P.M., and Hefter, G., *Ind. Eng. Chem. Res.*, 2005, vol. 44, no. 15, p. 5805.
57. Königsberger, E., May, P.M., and Hefter, G., *Monatsh. Chem.*, 2006, vol. 137, no. 9, p. 1139.
58. Li, X., Yan, L., Zhou, Q., Liu, G., and Peng, Z., *Trans. Nonferrous Met. Soc. China*, 2012, vol. 22, no. 2, p. 447.
59. Lainer, A.I., Eremin, N.I., Lainer, A.Yu., and Pevzner, I.Z., *Proizvodstvo glinozema: uchebnoe posobie dlya VUZov* (Alumina Production: Textbook for Higher School), Moscow: Metallurgiya, 1978.
60. Rayzman, V., Filipovich, I., Nisse, L., and Vlasenko, Y., *J. Miner. Met. Mater. Soc.*, 1998, vol. 50, no. 11, p. 32.
61. Apps, J.A. and Neil, J.M., Solubilities of aluminum hydroxides and oxyhydroxides in alkaline solutions, in *Chemical Modeling of Aqueous Systems II*, Melchior, D.C. and Bassett, R.L., Eds., Washington, DC: Am. Chem. Soc., 1990.
62. Nortier, P., Chagnon, P., and Lewis, A.E., *Chem. Eng. Sci.*, 2011, vol. 66, no. 12, p. 2596.
63. Qiu, G. and Chen, N., *Can. Metall. Q.*, 1997, vol. 36, no. 2, p. 111.
64. Zhang, Yi., Li, Y., and Zhang, Y., *J. Chem. Eng. Data*, 2003, vol. 48, no. 3, p. 617.
65. Ma, S., Zheng, S., Zhang, Yi., and Zhang, Y., *J. Chem. Eng. Data*, 2007, vol. 52, no. 1, p. 77.
66. Jin, W., Zheng, S., Du, H., Xu, H., Wang, S., and Zhang, Y., *J. Chem. Eng. Data*, 2010, vol. 55, no. 7, p. 2470.
67. Morachevskii, A.G. and Kokhatskaya, M.S., *Prikladnaya khimicheskaya termodinamika* (Applied Chemical Thermodynamics), St. Petersburg: St. Petersburg. Gos. Polithekh. Univ., 2008.
68. Dean, J.A., *Lange's Handbook of Chemistry*, New York: McGraw-Hill, 1999, p. 521.
69. Fricke, R. and Jucaitis, P., *Z. Anorg. Allg. Chem.*, 1930, vol. 191, p. 129.
70. Singh, S.S., *Soil Sci. Soc. Am. J.*, 1974, vol. 38, no. 3, p. 415.
71. Wesolowski, D.J., *Geochim. Cosmochim. Acta*, 1992, vol. 56, no. 3, p. 1065.
72. Castet, S., Dandurand, J.-L., Schott, J., and Gout, R., *Geochim. Cosmochim. Acta*, 1993, vol. 57, no. 20, p. 4869.
73. Bourcier, W.L., Knauss, K.G., and Jackson, K.J., *Geochim. Cosmochim. Acta*, 1993, vol. 57, no. 4, p. 747.
74. Benezeth, P., Palmer, D.A., and Wesolowski, D.J., *Geochim. Cosmochim. Acta*, 2001, vol. 65, no. 13, p. 2097.

Translated by Z. Smirnova